THE ASTROPHYSICAL JOURNAL, 419:30–46, 1993 December 10

DYNAMICS OF BINARY GALAXIES. I. WIDE PAIRS

JAYARAM N. CHENGALUR,[1] E. E. SALPETER,[2] AND YERVANT TERZIAN[1]
Received 1992 December 28; accepted 1993 June 18

ABSTRACT

We analyze pairs of galaxies selected from the CfA magnitude limited and SSRS diameter-limited redshift catalogs. The pairs are chosen only from regions of low galaxy density and have projected separations of up to 1.0 Mpc. This is almost an order of magnitude larger than the typical projected separations of samples of binary galaxies used in earlier studies.

Accurate H I velocities for these pairs were obtained at both Arecibo and Parkes Observatories, and we tabulate these new velocities along with total H I flux and other quantities of interest. The velocity measurements are very homogeneous, and we estimate the typical internal error in the measured systemic velocity to be under 5 km s^{-1}.

The velocity difference distribution $f(\Delta V)$ for our sample of isolated wide pairs of galaxies decreases monotonically with increasing velocity difference ΔV. In particular, we do not find a peak near 70 km s^{-1} as seen in earlier, more compact samples. This tends to confirm the suggestion of Schneider & Salpeter (1992) that the nonmonotonicity of earlier samples of binary galaxies is a consequence of a selection bias.

The distribution of ΔV for galaxy pairs in low-density regions is found to have two components, a peak around zero and a tail extending to larger velocity differences. The tail of the ΔV distribution has a strong dependence on the degree of isolation. As the stringency of the isolation criterion is increased, pairs are preferentially lost from the tail of the distribution. The width of the peak around zero, on the other hand, has little dependence on the isolation criterion.

For our sample of isolated pairs of galaxies, the median of the velocity differences is $\sim$30 km s^{-1}. The velocity difference of the galaxy pairs decreases with increasing projected separation. The characteristic 30 km s^{-1} velocity difference for our isolated sample is less than half the typical $\sim$70 km s^{-1} velocity difference found in previous studies using relatively compact pairs. We thus confirm the suggestion of Charlton & Salpeter (1991) that there exist physically associated galaxy pairs even at separations as large as 1.0 Mpc.

Unlike earlier samples of binary galaxies, the crossing time $r_p/\Delta V$ for our pairs is comparable to the Hubble time, so unique mass derivations are not possible. We nonetheless compute the dynamical mass of the galaxies as given by a variety of estimators, to get values of up to a few times 10^{12} $M_\odot$. This is consistent with both dynamical mass estimates for the Local Group, and also the recent mass estimates of spiral galaxies from the dynamics of faint satellites by Zaritsky et al. (1993).

Subject headings: galaxies: clustering — galaxies: distances and redshifts

1. INTRODUCTION

Evidence has been mounting that dark matter forms an important dynamic constituent of the universe for size scales ranging from galactic to the scale of clusters of galaxies. For galactic scales, the best evidence is from the flat rotation curves of spiral galaxies. On slightly larger scales, the presence of dark matter can be inferred from the dynamics of binary galaxies and small groups, e.g., Page (1958), Karachentsev (1972), Turner (1976), Peterson (1979), White (1981), van Moorsel (1982), White et al. (1983), Schneider et al. (1986), Schweizer (1988), Soares (1990), Sharp (1990), Charlton & Salpeter (1991), and Schneider & Salpeter (1992).

Most previous samples of binary galaxies were chosen from optical sky survey plates without a priori knowledge of the redshifts. Without redshift information it is difficult to find wide isolated pairs of galaxies. Wide pairs are likely to have a background galaxy projected between the pair, or generally at a small angular separation from the galaxies in the pair, and will hence be regarded as triplets and not pairs. Earlier samples have hence been restricted to relatively compact pairs, with typical separations of about 100 kpc.

Redshifts are now available for a statistically complete sample of galaxies, thanks to the recent large-scale redshift surveys. By using redshift information to define the binary galaxy sample, projection effects can be resolved, and there is no longer a strong selection bias against wide pairs. This method has been used by Rivolo & Yahil (1981) to study pairs from the Revised Shapely-Ames catalog, and by Charlton & Salpeter (1991) to study pairs from the considerably deeper CfA (Huchra et al. 1983) and SSRS (da Costa et al. 1988, 1991) catalogs. From the three-dimensional positional information in complete redshift catalogs, one can also compute the local galaxy density in a completely objective fashion. In regions of high density, two galaxies close in redshift space could be far apart in real space and appear close in redshift space only because they have large peculiar velocities. In selecting binary galaxies it is hence important to separate the low and high galaxy density regions.

Two recent studies suggest the presence of a population of wide, physically associated, galaxy pairs that has not been hitherto directly observed. (1) Charlton & Salpeter (1991) analyzed pairs from the CfA and SSRS catalogs and found an excess over background of pairs of galaxies in low-density

[1] Department of Astronomy and National Astronomy and Ionosphere Center, Cornell University, Ithaca, NY 14853.
[2] Department of Astronomy and Center for Radio Physics and Space Research, Cornell University, Ithaca, NY 14853.

regions even at projected separations are large as 1.0 Mpc. This is an order of magnitude larger than the physical separations of earlier samples. (2) From simple geometric considerations (Tifft 1977; see also § 5.1), it follows that the velocity difference distribution $f(\Delta V)$ for galaxy pairs must decrease monotonically with increasing velocity difference ΔV. The observed distribution has, however, been the subject of considerable controversy and has even led to claims of periodicity and nonconventional dynamics (Tifft 1980, Tifft 1982a, 1982b, Cocke & Tifft 1983, Tifft & Cocke 1987, Tifft & Cocke 1989). Schneider & Salpeter (1992) suggest that the velocity distributions of earlier samples of binary galaxies can be explained by conventional dynamics provided that there is a significant population of binaries with wide separations which are excluded from the earler samples because of their incompleteness beyond ~ 100 kpc.

Due to the routine nature of the redshift measurements, typical velocity errors in the redshift catalogs are ~ 30 km s^{-1}. This is of course negligible in studies of large-scale structure but could well be comparable to the velocity difference for wide isolated pairs of galaxies. For typical galaxy masses, pairs with separations ~ 1.0 Mpc might be near turnaround (Schneider & Salpeter 1992) and would hence have very small relative velocities. These small relative velocities would be completely dominated by the observation errors. Neutral hydrogen measurements, however, can easily provide sufficiently accurate velocity measurements.

In this paper we analyze a sample of binary galaxies chosen from the CfA and SSRS catalogs. The selected pairs lie in regions of low galaxy density and have projected separations of up to 1 Mpc. New, homogeneous H I velocities for 118 galaxies were obtained at both Arecibo Observatory and Parkes Observatory. Six pairs with very small separations were mapped at the VLA. Here we discuss only the wide pairs. The results of the mapping of close pairs will appear in a separate paper (Chengalur, Salpeter, & Terzian 1993). This study differs from earlier studies of binary galaxies in three important ways: (1) The sample extends to an order of magnitude larger separation than earlier studies, (2) pairs are strictly confined to regions of low local galaxy density, and (3) we study pairs chosen using a variety of isolation criteria and can hence estimate the importance of isolation criteria on the dynamics of galaxy pairs.

We will address several questions.

1. Does the inclusion of wide, (i.e., $r_p \sim 1$ Mpc), pairs of galaxies change the shape of the velocity difference distribution $f(\Delta V)$? In particular, does the inclusion of these pairs make the distribution monotonic, as predicted by Schneider & Salpeter (1992)?

2. What is the characteristic relative velocity of isolated wide pairs? Is there any evidence that wide pairs are close to turnaround? Note that the characteristic velocity difference of our wide pairs is related to the average peculiar velocity of field galaxies. The peculiar velocity of field galaxies has a bearing on both the virialization radius of clusters formed by the "raining in" of these galaxies, and cosmological models of galaxy creation. For example, explosive scenarios of galaxy formation lead to bound pairs with typical relative velocity of 200 km s^{-1} (Ostriker & Cowie 1980).

3. What is the effect of isolation? Do isolated low-density galaxy pairs have different characteristic velocities from galaxy pairs that are not isolated?

4. What are the characteristic masses of galaxies? Does this mass correlate with any other galaxy properties such as the luminosity or the rotation velocity?

5. What is the characteristic size of the dark halo of an individual galaxy?

In § 2 we describe the sample selection criteria. The observations are described in § 3, and the results presented in § 4. In § 5 we compare our results with those for earlier samples of more compact pairs. Section 6 is a collection of simple dynamic mass formulae. Statistics of the observed data and the results of applying the mass formulae to our data is discussed in § 7.

2. SAMPLE SELECTION

Most earlier studies of binary galaxies were restricted to relatively compact pairs, because of the difficulty of identifying wider pairs without redshift information. Furthermore, even samples of pairs with small angular separation contained spurious pairs, i.e., pairs which are close together only when viewed in projection. After obtaining redshifts for the entire sample, pairs with a very large redshift difference were rejected as being spurious. The exact threshold velocity difference beyond which two galaxies were regarded as being physically unrelated was set in a more or less ad hoc manner, based solely on the properties of the relatively small number of observed pairs.

From the redshift catalogs it is possible to compute the distribution function of pairs as a function of the radial velocity difference and projected separation $G(r_p, \Delta V)$. Charlton & Salpeter (1991) computed this distribution for pairs of galaxies from the CfA and SSRS catalogs separately for regions of low and high galaxy density. They found an excess over background of pairs of galaxies with projected separations less than 1.0 Mpc and velocity differences less than 150 km s^{-1}. In selecting binary galaxies we have been guided by this result.

The first step in choosing the sample of binary galaxies is the division of the total galaxy sample into regions of low and high galaxy density. Since the sample is being drawn from statistically complete redshift surveys, high galaxy density regions can be identified in a completely objective fashion. We choose to follow a prescription very similar to that used by Charlton & Salpeter (1991): for every galaxy in the sample, we count the number of other galaxies which have a projected separation of less than 4.5 Mpc from the target galaxy and which also have a redshift within 335 km s^{-1} of the target galaxy. The projected separation is converted from angular units to a linear dimension by assuming a Hubble constant of 75 km s^{-1} Mpc^{-1}. We will use this value for the Hubble constant throughout. Since the typical core dimensions of a galaxy cluster is about 1 Mpc, by using a value as large as 4.5 Mpc, we discriminate not just against cluster cores but also against cluster edges.

In order to estimate the galaxy density, the raw count of neighbors needs to be corrected for two reasons. The first is that the target galaxy may lie near the boundaries of the survey, and hence part of the "galaxy counting volume," falls outside the survey. In this case the local galaxy count is underestimated and should be corrected by the ratio of the total "galaxy counting volume" to the volume that is inside the survey. The other is that the survey gets increasingly incomplete with increasing redshift. This increasing incompleteness can be characterized by a selection function. The selection function, assumed to depend only on the redshift, gives the ratio of galaxies at a given redshift that are included in the sample to the total number of galaxies at that redshift. For example, in a magnitude-limited survey, the selection function depends on the luminosity function of the galaxies, and the magnitude limit used. The respective selection functions for the CfA and the SSRS catalogs have been computed by Charlton

(J. Charlton, private communication, but see also Charlton & Salpeter 1991), and we use them to further correct the galaxy count. When either one of these two corrections becomes very large, our estimate of the galaxy density will be badly affected by the statistics of small numbers. We hence exclude all galaxies which are so close to the edge that more than half the "galaxy counting volume" lies outside the survey boundaries, and also galaxies at redshifts beyond which the selection function falls to a value less than 0.1. We also use only those galaxies with redshift larger than 1100 km s^{-1} in order to minimize ambiguities introduced by the Virgocentric infall.

Clearly, galaxies with high corrected neighbor counts lie in clusters (or at the edges of clusters) and need to be excluded. There is a tradeoff involved in choosing the threshold density at which to make the cutoff. If the threshold is set too high, then the final binary galaxy sample will contain pairs whose dynamics is not dominated by mutual gravitational attraction. On the other hand, if it is set too low, then there will be insufficient galaxies left to do a sensible statistical study. The median density of the entire redshift catalog turns out to be a reasonable compromise. For example, with the cutoff at this density, all the members of the Eridanus group (Huchra & Geller 1982) are excluded from the low-density region. Similarly, all except one (NGC 1404) of the members of the Fornax group (Huchra & Geller 1982) are rejected from the low-density region. NGC 1404 is on the edge of the Fornax group and has a local galaxy density which is just slightly below the threshold.

Binary galaxies were then chosen from the low-density region Our sample includes pairs with projected separations less than 1.0 Mpc and velocity differences less than 400 km s^{-1}. Since we wish to make H I observations, we further restrict the sample to pairs in which both galaxies in the pair are of type Sa or later.

We use a variety of isolation criteria to divide this sample into smaller subsamples. These subsamples are analyzed separately, and we are particularly interested in the evolution of the pair properties with increasingly stringent isolation criteria. Using pairs with velocity differences up to 400 km s^{-1} (instead of Charlton & Salpeter's value of 150 km s^{-1}) serves two purposes: (1) It allows direct comparison of our histograms with those from earlier samples for which there have been claims of peaks at 140 km s^{-1} and 210 km s^{-1} (see for example, Tifft 1980), and (2) it allows us to establish the background level.

3. OBSERVATIONS AND DATA REDUCTION

Observations were made using the Arecibo 305 m radio telescope for galaxies from the CfA survey and the Parkes 64 m radio telescope for galaxies from the SSRS. Six galaxy pairs with particularly small angular separation were mapped at the VLA. In this paper we will discuss only the results from the single-dish observations.

At both Arecibo and Parkes, we used a total power, position-switching observing mode. At Atecibo we used both the manually tunable "21 cm" feed and the automatically tunable "22 cm" feed. The data were calibrated and corrected for the zenith angle dependence of the telescope gain using standard routines in the Arecibo data reduction package GALPAC. Since we were more interested in the systemic velocity than the total H I content, and since accurate flux calibration at Arecibo is not trivial, we do not expect that the flux calibration is accurate to better than 20%. The observation bandwidth was 10 MHz. A few galaxies at the start of the run were observed with a frequency resolution of 39.1 kHz (8 km s^{-1}), but the majority were observed at a frequency resolution of 19.6 kHz (4 km s^{-1}). All galaxy pairs regardless of their angular separation were observed. Since the telescope beam at these frequencies is about 3.'3, the closest galaxy pairs have spectra that are blended with one another. We flag cases in which the blending prevents us from determining the velocities accurately.

At Parkes the bandwidth used was once again 10 MHz, but the lower telescope gain forced us to use the lower frequency resolution, viz., 39.1 kHz (8 km s^{-1}). The smaller Parkes telescope also has a larger beam, and we did not observe pairs with angular separation less than 10', since the spectra of these galaxies are almost certainly guaranteed to be blended. Also the on-source time for each galaxy was 20 minutes, 4 times longer than the typical observation period at Arecibo. The longer observing time per galaxy made it impractical to observe the entire sample. Consequently, we only observed galaxies in pairs with projected separation less than 1.0 Mpc and $\Delta V \leq 200$ km s^{-1}, and which satisfied a moderate isolation criterion, i.e., at least one galaxy in the pair had no third galaxy (other than its paired partner galaxy) within a projected separation of 0.75 Mpc and a velocity difference of 300 km s^{-1}. Flux calibration is once again probably good to about 20%. We flag cases in which we feel the spectrum is not of sufficient quality to enable accurate velocity determination.

To ensure the maximum possible homogeneity of the data, we followed data reduction steps that were as uniform as possible. After the Parkes data were calibrated, they were converted to FITS format using routines in the Parkes software package SLAP. The data were then converted into the correct format for GALPAC, using software specifically written by us, and all subsequent reduction was done in GALPAC. Thus, apart from flux calibration, the data reduction for both the Arecibo and the Parkes data was identical.

In GALPAC, the final data reduction steps were as follows: each galaxy spectrum was baselined, with the emission-free region of the spectrum used to determine the baseline. Multiple observations of the same galaxy were averaged before baselining, provided that the observations used the same bandwidth and resolution. (We also checked the effect of removing the baseline before averaging; the difference was minimal.) There are a number of methods that have been used to identify the systematic velocity of a galaxy from its spectrum. For example, one could use the average of the peak velocities of the two horns in the profile, or the average of the velocities of the 20% points of the profile, etc. Each method has its own advantages and disadvantages, and varying levels of physical justification. For our purpose, the exact method used is not particularly important, provided (1) the same method is used consistently for all galaxies and (2) the method is not very susceptible to noise.

After some experimentation, we used the following method. The edges of the profile were fitted with straight lines (or a quadratic in the rare cases for which a straight line was a poor fit), and the point with emission equal to 50% of the peak emission on that half of the profile was located by interpolation along this line (quadratic). The systemic velocity was taken to be the mean of the velocities of the two 50% points. The error in our velocity measurement was estimated from the slope of the line and the rms noise in the baseline. A similar procedure was used by Schneider et al. (1986), and the reader is

1993ApJ...419...30C

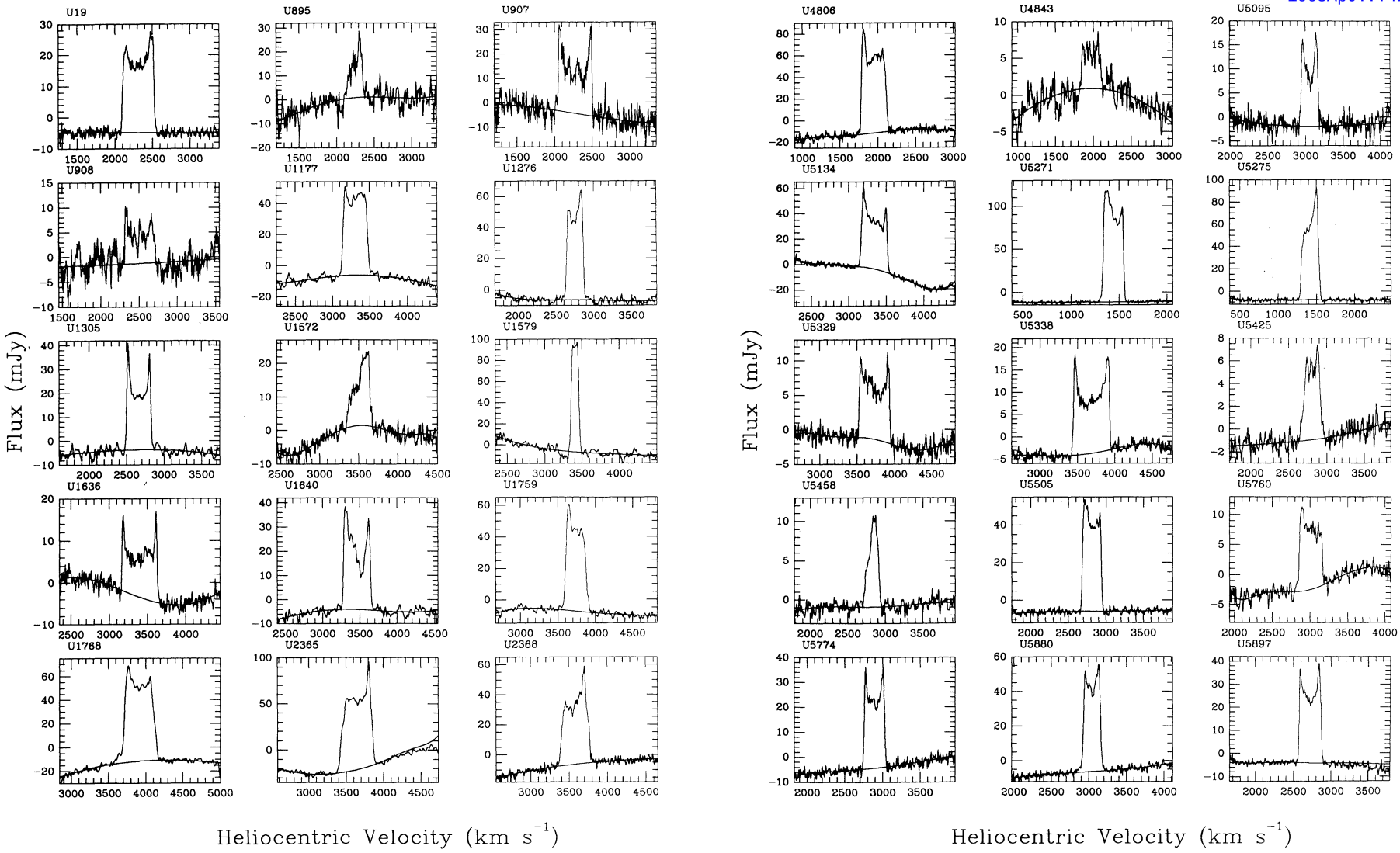

FIG. 1a

FIG. 1.—(*a*) Smoothed spectra for all the galaxies observed at Arecibo Observatory. The solid line is the baseline fitted to the spectrum before velocity measurements The *X*-axis is the heliocentric velocity, and the *Y*-axis is the flux in mJy. (*b*) Smoothed spectra for all the galaxies observed at Parkes Observatory. The solid line is the baseline fitted to the spectrum before velocity measurements. The *X*-axis is the heliocentric velocity, and the *Y*-axis is the flux in mJy.

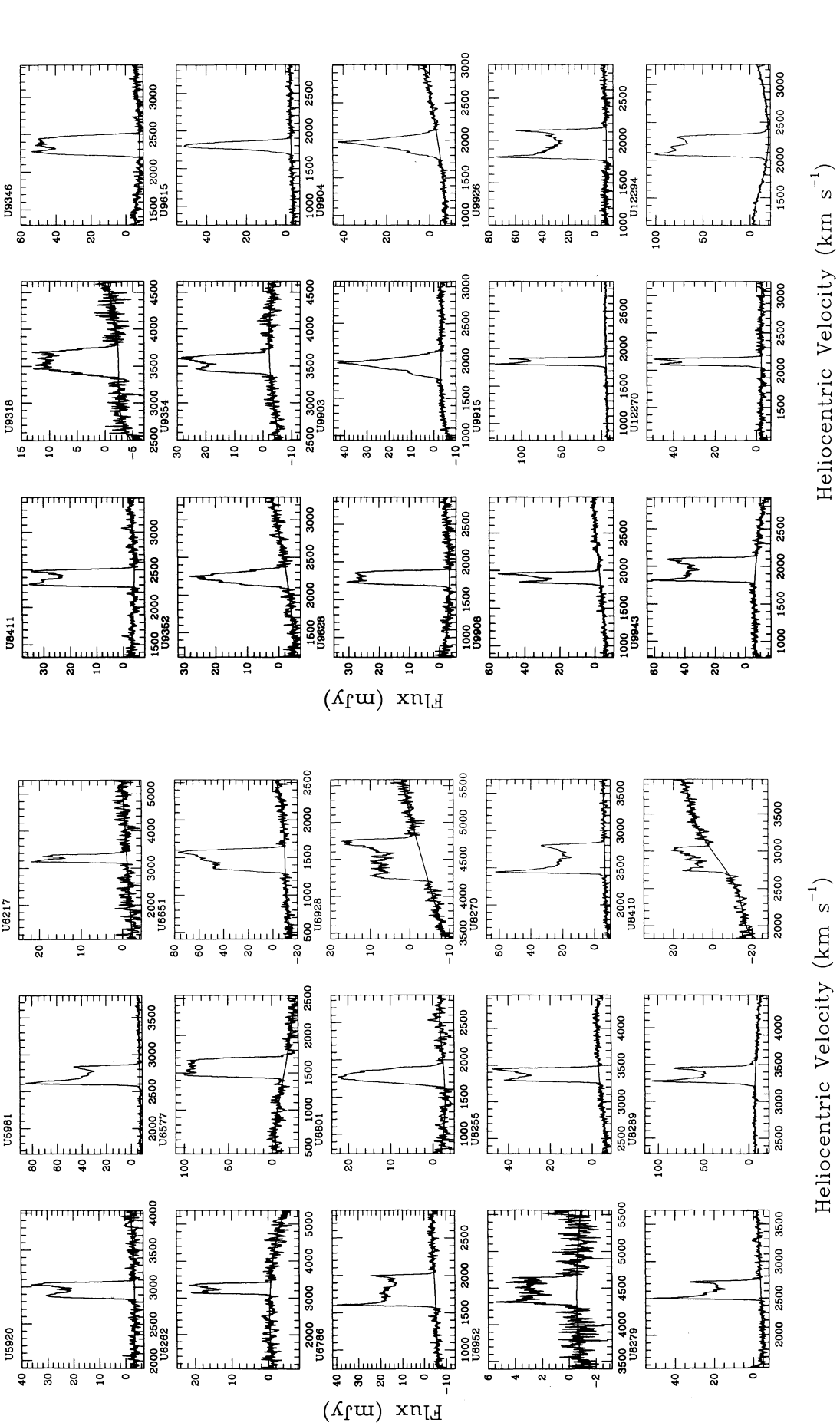

FIG. 1*a*—*Continued*

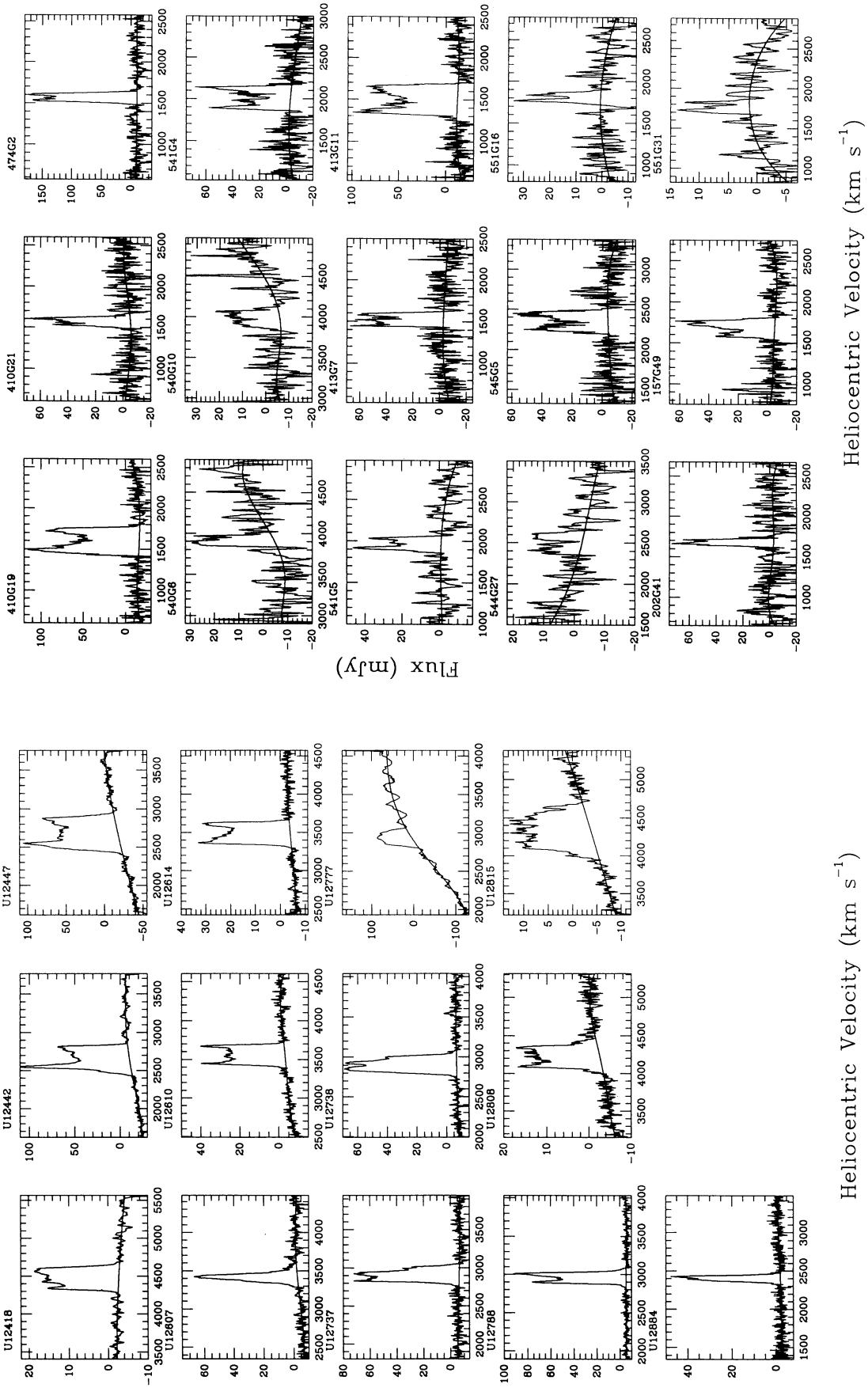

FIG. 1a—*Continued*

FIG. 1*b*

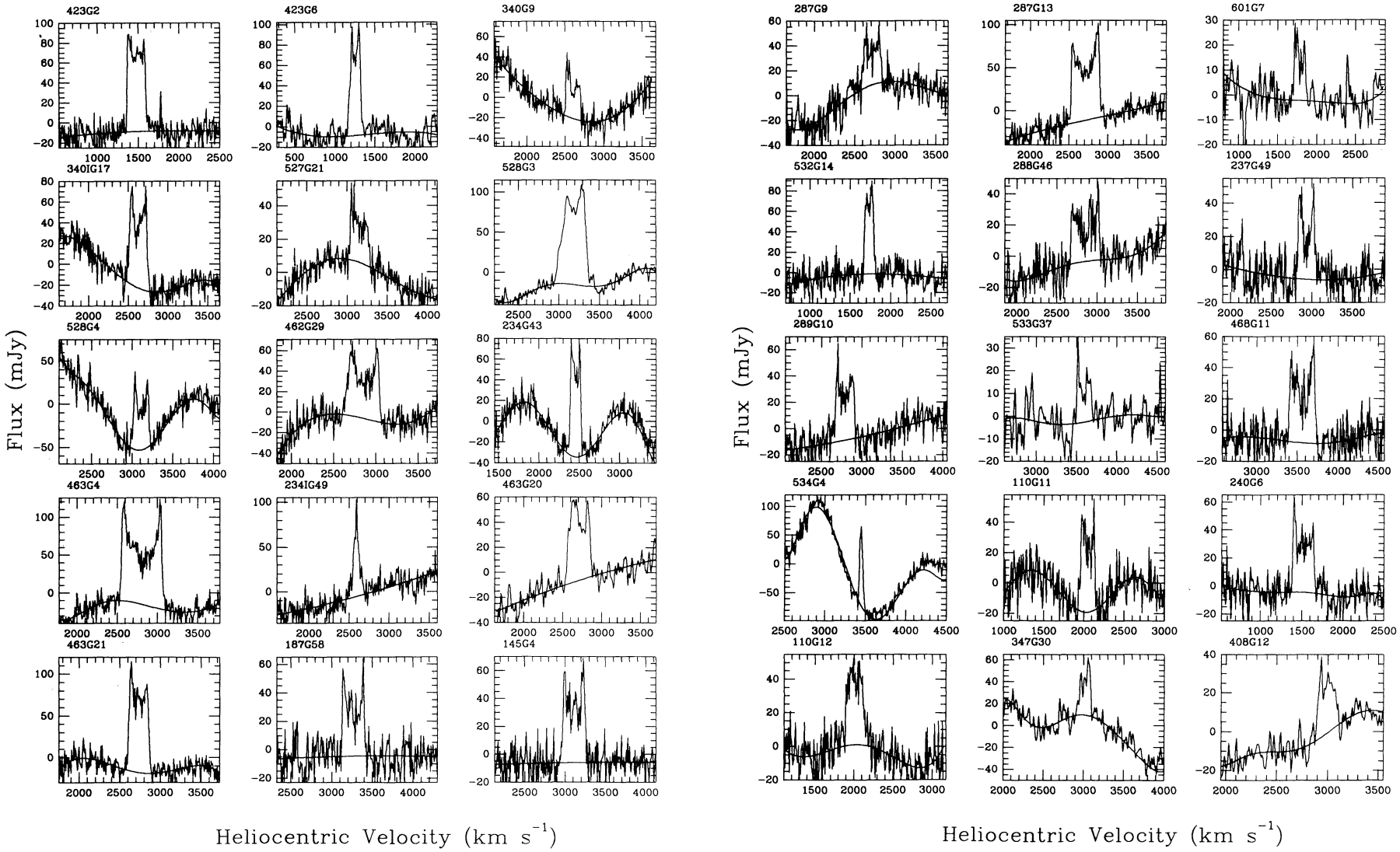

FIG. 1*b*—*Continued*

referred there (and to Schneider 1985) for a more detailed discussion of this velocity measurement method and the error estimation procedure. The fitting and measuring routines were developed by us specifically for this project, but are now a part of the standard Arecibo data reduction facility GALPAC. Note that the error in the velocity is a purely formal internal error and in most cases is likely to be an underestimate of the true error.

4. RESULTS OF THE OBSERVATIONS

4.1. *Neutral Hydrogen Data for Individual Galaxies*

The spectra of all the observed galaxies are shown in Figure 1, the velocities and other parameters are listed in Tables 1A and 1B. The spectra are arranged in order of increasing 1950 epoch right ascension. The various columns in Table 1 are as follows:

Column (1).—The name of the galaxy. UGC name is given for galaxies in the north, and the ESO name is given for galaxies in the south. An asterisk after the galaxy name implies that the spectrum is confused.

Column (2).—The 1950 epoch right ascension of the galaxy. These coordinates are those used during the observations and are either taken from the published literature or are from measurements from the optical plates.

Column (3).—The 1950 epoch declination of the galaxy. These coordinates are those used during the observations and are either taken from the published literature or are from measurements from the optical plates.

Column (4).—The systematic velocity (in km s^{-1}) of the galaxy as measured by us.

Column (5).—The *estimated internal error* (in km s^{-1}) for the galaxy's systematic velocity.

Column (6).—The integrated flux for the H I emission, in units of mJy km s^{-1}.

Column (7).—The width of the H I profile in km s^{-1}.

Column (8).—The peak flux of the H I profile in mJy.

Column (9).—The rms noise level in the baseline of the profile, in mJy. Note that the noise level is estimated after fitting a baseline to the profile. If the measurements are the average of observations with different frequency resolutions no noise level is listed.

Table 1A and Figure 1*a* are for the northern galaxies observed at Arecibo, while Table 1B and Figure 1*b* are for southern galaxies observed at Parkes.

4.2. *Quality of the Velocity Measurements*

For the northern sample, we have observed at Arecibo all bur seven (of a total of 57) galaxy pairs with velocity difference less than 200 km s^{-1} and projected separation less than 1.0 Mpc, regardless of isolation. H I velocities for six of these pairs were taken from the published literature or Haynes & Giovanelli (1992). We add to this sample, galaxy pairs with separations less than a Mpc, but with velocity differences between 200 km s^{-1} to 400 km s^{-1}. Some of these galaxies have been observed by us, and for the rest we use velocities either from the published literature, or from Haynes & Giovanelli (1992). We term the entire sample as being "not isolated." We also analyze different subsamples with varying isolation criteria but focus principally on pairs for which there is no third galaxy within 0.75 Mpc and 300 km s^{-1} of either galaxy in the pair; we call this sample the "isolated pairs." For samples with other isolation criteria we will specify the criteria explicitly. We have observed all the northern "isolated pairs" with $\Delta V \leq 200$ km s^{-1} at Arecibo.

For the southern galaxies we have H I data only for pairs for which at least one galaxy has no third galaxy (apart from its paired partner galaxy) within 0.75 Mpc and 300 km s^{-1}, and with pair velocity difference less than 200 km s^{-1} and projected separation less than 1.0 Mpc. We add to this sample isolated galaxy pairs with separations less than a 1.0 Mpc and velocity differences between 200 km s^{-1} and 300 km s^{-1}, where the velocities are from the SSRS. At this large velocity difference, the larger measurement error of the optical catalogs is not so significant. We also divide the sample into subsamples and will use the same nomenclature as for the Arecibo pairs.

Data for all the "isolated pairs" with $\Delta V \leq 200$ km s^{-1} and for which we have good H I observations are listed in Table 2. There are 32 such pairs. Note that not all the galaxies included in Table 1 appear in Table 2. Galaxies with confused H I profiles, or which are not part of a pair which has no third galaxy within 0.75 Mpc and 300 km s^{-1} of both galaxies in the pair, are excluded. The columns are as follows:

Column (1).—Name of the galaxy (UGC/ESO).

Column (2).—Inclination-corrected velocity width of the galaxy profile. The inclination is computed from the axis ratio of the galaxy using the standard formula $\cos^2 i = (r^2 - r_0^2)/(1.0 - r_0^2)$, where r is the axis ratio and $r_0 = 0.2$ is the assumed intrinsic disk thickness ratio. The axis ratio is taken from the RC3 (de Vaucouleurs et al. 1992) and is on a uniform scale for both the northern and the southern galaxies.

Column (3).—The luminosity of the galaxy in units of 10^9 $L_\odot$. The luminosity is computed using the B_T magnitudes from the RC3 (de Vaucouleurs et al. 1992) and is on a uniform scale for both the northern and southern galaxies and includes corrections for both galactic and internal absorption.

Column (4).—The radial velocity difference of the galaxy pair, in units of km s^{-1}.

Column (5).—The angular separation of the galaxy pair, in units of arcminutes.

Column (6).—The projected separation of the galaxy pair, in units of kpc.

Column (7).—R_0 defined as $[(\mathrm{Lum}_1 + \mathrm{Lum}_2/(\pi \times \Sigma)]^{1/2}$, where Σ is a constant surface brightness. R_0 is in units of kpc.

Column (8).—$W_0 = (W_1^4 + W_2^4)^{1/4}$, where W_1 and W_2 are the inclination-corrected velocity widths of the individual galaxies.

Apart from one galaxy (UGC 8410), for which the optical velocity listed in the CfA is 2583 km s^{-1} while the H I velocity is 2892 km s^{-1}, there is no severe disagreement between the optical velocities and the H I velocities. While this is reassuring, what we really need to ensure is that our velocity accuracies are indeed a few km s^{-1}. A simple external check as to the quality of our data is to compare the median velocities for the pairs as computed from the original optical catalog against those from the new H I observations. We use the sample for which we have the most complete new measurements, viz., the isolated pairs with velocity difference less than 200 km s^{-1}. For the pairs in the north (i.e., from the CfA catalog), the median velocity difference from the old measurements is 30 km s^{-1} while the corresponding figure from our own measurements is 26 km s^{-1}. In the CfA catalog, existing H I velocity measurements were used, if available, and most of our galaxies have published H I velocity measurements. A much more striking confirmation of the value of H I observations comes from the comparison for the southern galaxies, where there are far fewer

TABLE 1A

GALAXIES OBSERVED AT ARECIBO[a]

Name (UGC) (1)	R.A. (1950) (2)	Decl. (1950) (3)	Velocity (km s^{-1}) (4)	V_{err}[b] (km s^{-1}) (5)	Integrated Flux (mJy km s^{-1}) (6)	Width (km s^{-1}) (7)	Peak Flux (mJy) (8)	rms (mJy) (9)
U19	00^{h}01^{m}24^s.8	+20°28′18″	2309.0	0.7	0.1016E+05	415.6	32.5	1.1
U895	01 18 51.1	+06 45 25	2255.4	8.5	0.3392E+04	195.5	27.5	3.1
U907	01 19 11.1	+04 59 36	2270.5	1.5	0.1105E+05	451.5	47.2	...
U908	01 19 16.3	+08 56 40	2503.1	6.1	0.2674E+04	379.0	12.9	...
U1177	01 37 32.2	+05 28 30	3310.1	1.3	0.1719E+05	333.9	57.7	1.9
U1276	01 46 30.2	+20 27 48	2748.3	0.6	0.1355E+05	226.4	76.5	...
U1305	01 47 55.7	+21 30 45	2655.5	2.3	0.8890E+04	324.7	44.7	1.7
U1572	02 02 05.1	+08 18 17	3504.0	4.0	0.4242E+04	282.7	22.8	2.3
U1579	02 02 37.7	+05 51 56	3410.1	2.5	0.1087E+05	107.3	105.0	2.9
U1636	02 05 54.6	+06 05 06	3397.5	0.7	0.4854E+04	461.4	19.6	1.9
U1640	02 06 17.6	+07 44 08	3465.1	1.1	0.1019E+05	363.3	42.4	1.4
U1759	02 14 27.0	+14 19 05	3741.0	1.1	0.1543E+05	272.1	67.6	1.4
U1768	02 15 15.2	+14 19 01	3915.2	1.3	0.2812E+05	397.9	81.4	1.6
U2365	02 50 56.8	+12 48 43	3639.5	1.1	0.3323E+05	407.7	114.0	1.6
U2368	02 51 06.1	+12 38 43	3570.6	0.6	0.1538E+05	338.1	64.8	1.6
U4806	09 06 29.6	+33 19 38	1944.4	0.5	0.2417E+05	326.9	97.0	2.2
U4843	09 09 39.3	+35 07 57	1961.6	10.2	0.1359E+03	240.8	8.2	...
U5095	09 31 22.5	+09 42 13	3055.2	0.6	0.2652E+04	223.7	16.9	1.5
U5134	09 35 27.1	+09 45 00	3339.1	0.3	0.1487E+05	345.7	64.5	1.3
U5271	09 47 23.8	+13 03 00	1440.5	0.2	0.2346E+05	213.0	129.0	1.1
U5275	09 47 45.7	+13 00 06	1412.2	0.2	0.1660E+05	226.8	101.0	1.1
U5329	09 52 49.6	+16 40 13	3732.9	0.5	0.3130E+04	403.5	12.63	...
U5338	09 53 35.2	+17 04 11	3687.3	0.4	0.6839E+04	483.5	22.5	0.8
U5425	10 01 40.1	+13 52 00	2804.6	1.5	0.1546E+04	216.2	8.3	0.6
U5458	10 04 47.8	+12 30 59	2836.9	0.7	0.1651E+04	140.0	11.7	1.0
U5505	10 10 09.6	+12 55 00	2810.7	0.2	0.1258E+05	251.6	59.6	1.1
U5760	10 33 41.8	+13 58 17	3010.1	2.7	0.3292E+04	307.8	14.0	0.9
U5774	10 34 29.8	+12 54 47	2888.9	0.4	0.8232E+04	270.4	40.8	1.3
U5880	10 43 55.2	+14 00 54	3039.5	0.3	0.1226E+05	227.7	61.6	1.2
U5897	10 45 02.5	+11 20 34	2718.5	0.2	0.9638E+04	295.4	43.6	0.9
U5920	10 46 17.8	+14 29 00	2957.0	0.6	0.6784E+04	215.3	39.7	1.3
U5981	10 49 26.1	+10 24 33	2721.3	0.1	0.1428E+05	258.5	92.1	0.7
U6217	11 08 08.1	+12 17 21	3251.3	0.7	0.4289E+04	217.6	24.1	...
U6262	11 11 19.6	+12 34 29	3249.4	0.3	0.5276E+04	282.6	23.3	...
U6577	11 33 54.3	+36 41 15	1569.8	1.4	0.2815E+05	259.4	115.0	4.1
U6651	11 38 40.0	+36 49 27	1465.4	0.7	0.1980E+05	294.4	86.7	2.2
U6786	11 46 33.2	+27 18 06	1798.6	0.4	0.9987E+04	421.8	44.9	1.1
U6801	11 47 28.5	+26 45 27	1783.4	0.9	0.4635E+04	192.0	25.0	0.9
U6928	11 54 46.8	+25 28 23	4502.4	0.6	0.6715E+04	543.3	19.2	1.1
U6952	11 55 36.0	+25 24 00	4468.6	1.5	0.1369E+04	359.6	6.0	0.8
U8255	13 08 27.0	+11 44 26	3367.2	0.2	0.7915E+04	191.2	50.6	0.9
U8270	13 09 12.1	+23 11 03	2623.1	0.3	0.1364E+05	391.7	68.8	1.0
U8279	13 09 42.5	+24 21 42	2612.0	0.5	0.7425E+04	249.2	54.5	1.1
U8289	13 10 10.5	+12 52 13	3362.4	0.4	0.1708E+05	218.2	114.0	1.4
U8410	13 20 33.8	+27 14 30	2891.5	3.0	0.4868E+04	334.3	22.0	1.8
U8411	13 20 35.2	+28 34 43	2391.6	0.3	0.7463E+04	222.6	39.4	1.1
U9318	14 28 01.1	+31 26 11	3561.7	1.1	0.4424E+04	322.8	15.2	1.1
U9346	14 29 28.3	+06 28 18	2354.5	0.3	0.1468E+05	264.9	61.6	1.3
U9352	14 29 57.5	+08 18 05	2227.8	0.4	0.4634E+04	154.1	30.9	1.2
U9354	14 30 30.1	+31 53 25	3533.0	0.6	0.6170E+04	244.0	30.8	1.4
U9615	14 54 29.0	+30 26 03	1804.7	0.3	0.5912E+04	105.5	53.8	0.9
U9628	14 55 31.5	+30 10 06	1792.5	0.3	0.5636E+04	185.2	34.0	1.0
U9903*	15 32 13.1	+15 21 40	1965.1	0.3	0.7261E+04	136.1	46.4	0.9
U9904*	15 32 15.6	+15 22 10	1964.1	0.3	0.7128E+04	132.7	46.6	0.9
U9908	15 32 34.6	+11 54 53	1902.0	0.2	0.6226E+04	147.5	57.9	1.0
U9915	15 33 00.0	+12 12 59	1827.6	0.1	0.1162E+05	98.8	138.0	0.9
U9926	15 34 14.0	+16 46 23	1957.5	0.3	0.1674E+05	342.9	83.5	1.6
U9943	15 36 08.1	+12 21 00	1956.7	0.4	0.1558E+05	315.9	68.4	1.5
U12270	22 55 39.5	+14 02 14	2114.5	0.3	0.5306E+04	103.9	58.3	...
U12294	22 57 34.8	+15 42 50	2192.8	0.2	0.2379E+05	285.4	104.1	...
U12418	23 10 17.7	+12 24 30	4470.9	1.8	0.5509E+04	306.8	21.5	...
U12442*	23 12 01.8	+04 13 33	2675.6	0.9	0.2463E+05	314.1	121.0	1.8
U12447*	23 12 10.2	+04 15 43	2685.2	2.0	0.3747E+05	433.8	121.0	2.5
U12607	23 25 11.7	+23 18 51	3408.9	0.4	0.6745E+04	101.3	61.9	4.6
U12610	23 25 36.1	+23 15 18	3556.0	0.3	0.8321E+04	267.0	43.0	3.2
U12614	23 25 58.1	+22 08 50	3489.4	0.5	0.9612E+04	295.3	40.1	...
U12737*	23 38 55.6	+03 27 43	2911.9	45.8	0.1304E+05	205.2	78.7	2.7
U12738*	23 39 00.0	+03 26 50	2903.1	1.3	0.1418E+05	205.4	75.5	2.3

TABLE 1A—*Continued*

Name (UGC) (1)	R.A. (1950) (2)	Decl. (1950) (3)	Velocity (km s^{-1}) (4)	V_{err}[b] (km s^{-1}) (5)	Integrated Flux (mJy km s^{-1}) (6)	Width (km s^{-1}) (7)	Peak Flux (mJy) (8)	rms (mJy) (9)
U12777.....	23 44 04.2	+03 31 17	2928.0	12.1	0.1507E+05	199.5	82.9	8.3
U12788.....	23 46 11.5	+03 53 43	2953.5	0.5	0.1161E+05	147.8	97.3	1.7
U12808.....	23 48 31.5	+19 52 25	4221.2	0.9	0.5806E+04	316.0	21.3	1.8
U12815.....	23 48 52.2	+19 50 08	4318.0	16.0	0.7758E+04	605.9	16.6	1.1
U12884.....	23 56 51.6	+20 28 18	2401.0	0.7	0.3686E+04	80.8	49.7	1.8

[a] See text for explanation of columns.
[b] This is a formal internal error, which is likely to be an underestimate. We expect that our velocity accuracy is better than 5 km s^{-1} on average.

TABLE 1B

GALAXIES OBSERVED AT PARKES[a]

Name (UGC) (1)	R.A. (1950) (2)	Decl. (1950) (3)	Velocity (km s^{-1}) (4)	V_{err}[b] (km s^{-1}) (5)	Integrated Flux (mJy km s^{-1}) (6)	Width (km s^{-1}) (7)	Peak Flux (mJy) (8)	rms (mJy) (9)
410G19	00^{h}31^{m}47^s.0	−28°04′48″	1602.0	2.6	0.2907E+05	319.7	131.0	8.9
410G21	00 32 05.0	−30 17 42	1570.0	3.2	0.6377E+04	107.4	74.4	8.4
474G2.....	00 33 19.0	−25 38 54	1569.2	1.6	0.1987E+05	117.6	183.0	10.1
540G6.....	00 34 52.0	−20 12 42	3910.3	6.5	0.3008E+04	133.3	29.7	8.7
540G10	00 37 05.0	−20 39 30	3976.8	11.8	0.4161E+04	205.5	27.2	7.6
541G4.....	00 56 30.0	−19 00 48	2014.2	3.1	0.1070E+05	276.0	71.9	10.1
541G5.....	00 56 51.0	−20 50 54	1970.5	6.3	0.5175E+04	160.9	47.4	5.9
413G7.....	01 25 39.0	−29 20 42	1525.2	2.6	0.8610E+04	168.4	69.9	9.6
413G11	01 31 59.0	−29 40 30	1500.2	4.0	0.2811E+05	357.5	111.0	10.4
544G27	02 10 34.0	−19 32 54	2504.6	18.2	0.3168E+04	248.6	17.3	5.1
545G5.....	02 17 47.0	−19 58 48	2355.5	6.6	0.1088E+05	248.7	63.2	9.8
551G16	04 33 32.0	−22 05 24	1808.0	10.0	0.2713E+04	117.6	33.3	5.3
202G41	04 35 44.0	−52 16 30	1679.7	5.6	0.5586E+04	82.3	76.2	10.6
157G49	04 38 27.0	−53 06 30	1677.9	5.2	0.8962E+04	204.3	68.0	7.9
551G31	04 40 20.0	−21 47 06	1767.9	11.0	0.1190E+04	140.9	12.5	2.7
423G2.....	05 13 21.0	−30 35 00	1482.1	2.3	0.1908E+05	231.1	97.5	10.0
423G6.....	05 17 56.0	−32 11 30	1256.1	5.6	0.1300E+05	133.7	107.0	9.6
340G9.....	20 14 02.0	−38 49 48	2608.1	3.3	0.6823E+04	196.5	63.0	10.0
340IG17	20 16 22.0	−39 26 42	2628.8	4.3	0.1682E+05	224.6	101.0	9.6
527G21	20 20 56.0	−26 10 36	3155.7	5.9	0.6172E+04	226.4	46.6	6.4
528G3.....	20 22 08.0	−24 58 18	3158.6	9.1	0.3391E+05	312.6	126.0	6.3
528G4.....	20 22 20.0	−25 59 30	3112.2	5.7	0.1093E+05	189.2	89.9	10.9
462G29	20 28 33.0	−31 00 12	2853.3	7.3	0.1828E+05	371.8	73.1	10.9
234G43	20 28 40.0	−48 41 54	2457.2	2.8	0.1231E+05	133.0	111.0	9.4
463G4.....	20 31 14.0	−32 09 12	2804.2	3.8	0.4226E+05	501.8	144.0	10.0
234IG49	20 31 42.0	−50 02 12	2590.5	6.9	0.7412E+04	50.9	108.0	10.5
463G20	20 40 11.0	−30 02 00	2714.2	9.2	0.1551E+05	286.9	66.0	7.5
463G21*	20 40 31.0	−29 53 06	2735.4	3.7	0.2435E+05	245.2	132.0	9.5
187G58*	21 08 27.0	−57 29 00	3268.1	5.2	0.1037E+05	271.3	68.3	10.4
145G4.....	21 15 08.0	−57 51 06	3113.3	6.5	0.1290E+05	270.6	74.9	9.5
287G9.....	21 17 58.0	−46 21 54	2715.0	9.4	0.6967E+04	204.8	51.9	11.4
287G13	21 19 56.0	−45 59 12	2714.9	3.3	0.2705E+05	366.6	110.0	9.9
601G7.....	21 59 35.0	−21 16 54	1789.1	7.8	0.3091E+04	145.2	31.0	6.0
532G14	22 00 09.0	−22 42 48	1731.7	2.6	0.8638E+04	115.8	90.9	11.2
288G46	22 07 50.0	−46 19 42	2847.2	4.2	0.9212E+04	351.6	50.2	9.4
237G49	22 12 57.0	−47 54 42	2931.1	5.9	0.7359E+04	204.9	57.8	10.3
289G10	22 13 38.0	−47 22 06	2793.5	3.7	0.9726E+04	227.2	74.4	9.7
533G37	22 27 52.0	−27 11 18	3597.6	7.2	0.3499E+04	187.5	37.6	6.9
468G11	22 30 30.0	−27 30 18	3560.3	4.2	0.1227E+05	314.5	64.5	11.7
534G4.....	22 34 18.0	−25 29 48	3449.9	3.0	0.5844E+04	46.1	136.0	10.9
110G11	23 24 19.0	−65 32 48	2046.8	5.5	0.9223E+04	180.1	73.7	10.8
240G6.....	23 30 18.0	−51 58 24	1521.0	4.5	0.1035E+05	263.5	67.7	9.8
110G12	23 32 02.0	−65 40 24	2011.7	11.7	0.9535E+04	214.4	51.5	10.2
347G30	23 34 29.0	−37 59 30	3017.8	10.9	0.5232E+04	142.4	53.1	7.3
408G12	23 34 55.0	−37 16 24	2991.0	20.0	0.4929E+04	165.7	42.0	5.1

[a] See text for explanation of columns.
[b] This is a formal internal error, which is likely to be an underestimate. We expect that our velocity accuracy is better than 5 km s^{-1} on average.

TABLE 2

DATA FOR ISOLATED PAIRS[a]

Name (UGC/ESO) (1)	Corrected Width (km s^{-1}) (2)	Luminosity (10^a $L_\odot$) (3)	ΔV (km s^{-1}) (4)	Angular Separation (5)	R_p (kpc) (6)	R_0 (kpc) (7)	W_0 (km s^{-1}) (8)
U19	422.1	18.6					
U12884	193.0	7.4	92.0	64'.0	585	1.7	426.6
U907	659.1	32.4					
U895	202.4	4.1	15.1	105.9	930	2.0	660.6
U1636	490.7	6.9					
U1579	495.6	5.7	12.6	50.7	669	1.2	586.5
U1640	382.0	13.0					
U1572	286.2	9.6	38.9	71.2	963	1.6	409.1
U1768	598.3	38.7					
U1759	287.2	13.5	174.2	11.7	174	2.4	606.1
U2365	425.9	32.8					
U2368	525.5	10.2	68.9	10.3	144	2.2	574.8
U5271	241.2	4.1					
U5275	227.7	2.3	28.3	6.1	33	0.8	279.2
U5338	489.4	13.4					
U5329	453.5	10.9	45.6	26.3	378	1.6	561.9
U5505	274.0	9.5					
U5458	179.6	3.8	26.2	82.1	899	1.2	285.9
U5981	558.5	14.7					
U5897	310.6	9.1	2.8	85.6	903	1.6	571.4
U6262	301.8	8.6					
U6217	279.2	6.9	1.9	49.8	628	1.3	346.3
U6786	489.9	6.0					
U6801	225.2	2.9	15.2	34.9	242	1.0	495.3
U8270	469.3	11.9					
U8279	363.8	5.3	11.1	71.0	721	1.4	506.9
U8289	407.3	19.6					
U8255	297.2	6.1	4.8	72.3	944	1.7	433.5
U9318	471.2	15.2					
U9354	303.7	4.5	28.7	41.8	575	1.5	490.4
U9628	246.3	2.0					
U9615	227.9	1.2	12.2	20.9	146	0.6	282.6
U12607	242.0	12.8					
U12610	332.3	8.5	147.1	6.6	89	1.5	353.5
U12788	215.8	9.3					
U12777	227.7	8.2	25.5	38.9	443	1.4	264.0
U12815	650.0	27.6					
U12808	1043.8	22.9	96.8	5.4	90	2.3	1081.0
410G19	356.8	9.6					
474G2	167.2	2.9	32.8	147.3	906	1.2	361.0
540G6	265.8	19.2					
540G10	255.8	2.1	66.5	41.1	629	1.5	310.3
541G4	308.0	4.4					
541G5	186.9	0.4	43.7	110.2	852	0.7	317.9
413G11	537.6	20.1					
413G7	228.5	0.4	25.0	85.0	499	1.5	541.9

TABLE 2—*Continued*

Name (UGC/ESO) (1)	Corrected Width (km s^{-1}) (2)	Luminosity (10^a $L_\odot$) (3)	ΔV (km s^{-1}) (4)	Angular Separation (5)	R_p (kpc) (6)	R_0 (kpc) (7)	W_0 (km s^{-1}) (8)
157G49	205.4	1.8					
202G41	120.1	0.5	1.8	55.8	363	0.5	211.2
340IG17	233.2	10.4					
340G9	196.5	6.8	20.7	45.8	465	1.4	258.3
234IG49	121.6	5.9					
234G43	200.0	2.2	133.3	85.6	838	0.9	206.5
187G58	271.3	7.8					
145G4	272.4	7.5	154.8	58.0	718	1.3	323.3
287G13	373.6	15.5					
287G9	204.8	4.8	0.1	30.5	322	1.5	381.8
237G49	204.9	4.1					
289G10	227.2	3.8	137.6	33.3	370	0.9	257.9
468G11	339.0	13.2					
533G37	207.8	2.3	37.3	39.9	554	1.3	350.4
110G12	214.4	2.8					
110G11	231.1	1.9	35.1	48.4	381	0.7	265.4
347G30	239.5	10.1					
408G12	187.6	1.6	26.8	43.4	506	1.1	259.4

[a] See text for explanation of columns.

existing H I measurements. Using the SSRS catalog velocities, the median velocity difference for the southern galaxies is 64 km s^{-1}, while using our new H I velocities, the median velocity is just 35 km s^{-1}. Clearly, velocity measurement errors of as much as 30 km s^{-1}, while unimportant in studies of large-scale structure, are more than sufficient to dominate the true velocity difference in pairs. Since mass estimates depend on the square of the velocity difference, the importance of accurate velocity measurements cannot be overemphasized.

5. COMPARISON WITH EARLIER SAMPLES AND THE EFFECT OF ISOLATION CRITERIA

5.1. *Comparison with Earlier Samples*

From quite simple geometric considerations, it follows that the velocity distribution for a complete set of paired galaxies has to be monotonic (Tifft 1977). Briefly, the argument is as follows. Assume, for the moment, that all binary galaxies have a true spatial velocity difference, v. With the standard assumption that the pairs have no special orientation when viewed from Earth, the number of pairs for which the angle between their spatial velocity difference vector and the line of sight is between θ and $\theta + d\theta$ is given by $N(\theta) \propto \sin\theta\, d\theta$. Further these pairs will have an *observed radial velocity difference* $v_r = v\cos\theta$. The relation between the differential observed velocity and differential inclination angle, is hence $dv_r \propto \sin\theta\, d\theta$. Therefore, the number of pairs as a function of their velocity difference $N_1(v_r)$ is a constant in the interval $0 \le v_r \le v$. Now, the actual velocity distribution histogram from a sample of pairs with a variety of true spatial velocities can be viewed as a set of rectangles with one corner at the origin and widths equal to the true spatial velocity, stacked on top of one another. Clearly the sum of all these must decrease monotonically with increasing velocity. However, many earlier samples of binary galaxies did not have monotonically decreasing velocity histograms, (Tifft & Cocke 1989 and references therein), which Tifft and his coworkers explain by invoking a nonconventional origin for the redshift.

This nonmonotonicity could, however, have a more conventional explanation, namely that the observed sample of binary galaxies is not complete. This is the argument favored by Schneider & Salpeter (1992). They point out that if binary galaxies have largely radial orbits, and if the observed sample includes only relatively compact pairs, then the sample preferentially includes pairs with orientations aligned with the line of sight, and hence with large velocities. Pairs with orientations perpendicular to the line of sight and small velocity differences are excluded from the sample. The resulting velocity difference histogram for the sample will have peaks away from zero. This explanation was also recognized by Tifft (1977), but was rejected, presumably because there was no clear evidence for pairs of galaxies with wide separations. It is worth noting that in regions where multiple galaxy interactions are unimportant, and in the absence of some kind of primordial cosmic vorticity, wide pairs are likely to have more or less radial orbits. As the galaxies approach one another, their orbits could become circularized by dynamic friction. The eccentricity of the orbits of binary galaxies hence evolves with separation as discussed in more detail by Schneider & Salpeter (1992).

In our discussions, we will find it useful to compare the properties of our sample of binary galaxies with those used in earlier studies. For the comparison we will use primarily the robust sample used by Schneider & Salpeter (1992, hereafter SS). This sample is a compilation from the published literature of all pairs used in earlier studies of binary galaxies for which good quality H I velocities are available. Since the published literature includes pairs with a variety of selection criteria, this is not a uniform sample. However, SS do attempt to homoge-

nize the sample by applying their own relatively stringent selection criteria uniformly to the compiled sample. The SS sample is a collection of isolated binary galaxies, and hence the correct subsample to compare it against is our "isolated sample," i.e., those galaxies with no other galaxy within 0.75 Mpc and 300 km s^{-1}. The SS sample includes pairs with velocity differences up to 300 km s^{-1}, and so we too will consider pairs with velocity differences less than 300 km s^{-1}.

There are a total of 26 isolated pairs in the north and 34 isolated pairs in the south with $\Delta V \leq 300$ km s^{-1}. The projected separation distribution for these 60 pairs is shown in Figure 2*a*. The solid histogram is for those which we have good-quality velocities, while the dotted histogram is for the entire sample, regardless of the velocity accuracy. Apart from the shortest separations, where confusion prevents us from obtaining good velocities, the distributions are quite similar. The projected separation histograms of the SS sample is shown in Figure 2*b* and shows a strong cutoff above 100 kpc. Our own sample, which is chosen from redshift surveys (Fig. 2*a*), has a distribution which is more or less flat out to 1.0 Mpc, with, perhaps, a small peak at the smallest separations. This is essentially the same result as that found by Charlton & Salpeter (1991) and clearly illustrates the point that we have been emphasizing, viz., that pairs chosen from a redshift catalog are not biased toward small separations.

We want to compare our velocity difference distribution with that of SS and with the conjecture of periodic redshifts of Cocke & Tifft (1983). As emphasized by Newmann, Haynes, & Terzian (1989), in testing hypothesis on distribution shapes it is important to freeze the binning scheme *before* analyzing new data. We therefore follow SS in using the binning scheme suggested by Tifft & Cocke (1989), which has bins of nonuniform width. The number of pairs in each bin is scaled in inverse proportion to width of the bin so that the height of each bin remains proportional to the amplitude of the distribution function $f(\Delta V)$. The histogram for the SS sample is reproduced in Figure 3*a*. In their analysis, SS point out that the feature with the highest statistical significance is the dip in the third bin. As described above, they attribute this paucity of sources with small velocity difference to the lack of wide pairs, and they postulated, *even before the present data were gathered*, the existence of wide pairs of galaxies, for which the velocity difference distribution would be monotonic.

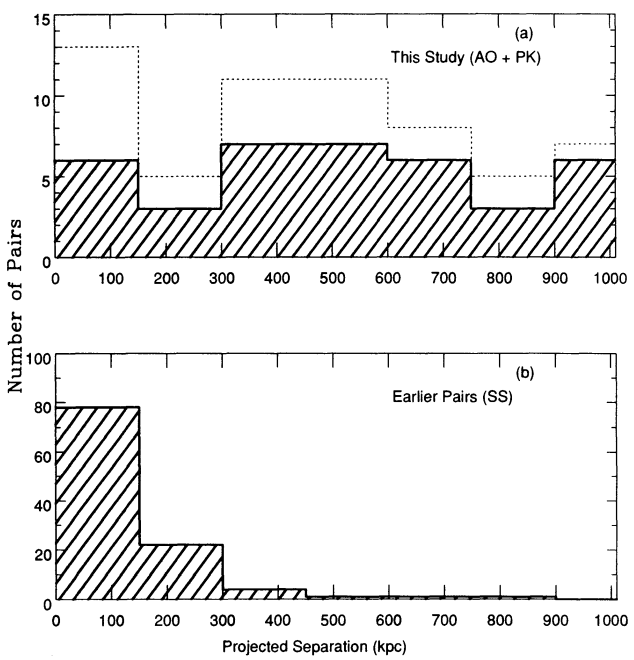

FIG. 2.—(*a*) The histogram of projected separations of the "isolated pairs" with $\Delta V \leq 300$ km s^{-1}, (i.e., the pairs with $r_p \leq 1.0$ Mpc, $\Delta V \leq 300$ km s^{-1}, and with no other galaxy within 0.75 Mpc and 300 km s^{-1} of either galaxy in the pair). The dotted histogram shows all pairs satisfying this criteria, the shaded histogram is for those pairs for which we have good velocity information. (*b*) The histogram of projected separations of the binary galaxy sample analyzed by Schneider & Salpeter (SS).

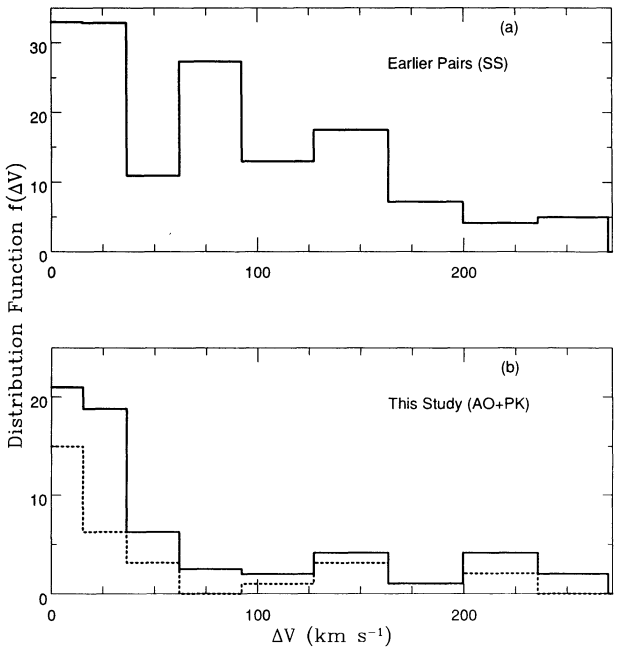

FIG. 3.—(*a*) The velocity difference distribution function for the sample of binary galaxies analyzed by Schneider & Salpeter (SS). The binning scheme is that advocated by Tifft & Cocke (1989) and used by Schneider & Salpeter (SS). (*b*) The velocity difference distribution function for the "isolated pairs" sample used in this study. Same binning scheme as for (*a*). The solid histogram is for the entire "isolated pairs" sample. The dashed histogram is for the subset for which the pairs have no fainter comparisons listed in the NED database (see § 5.3).

Figure 3*b* is the velocity difference distribution for the isolated Arecibo and Parkes pairs. The distribution is essentially monotonic, and in particular there is no longer a dip in the third bin and the fourth bin is quite low. The peak around zero ΔV is surprisingly narrow (e.g., the median of $\Delta V = 27.5$ for pairs with velocity difference up to 150 km s^{-1}). As mentioned, we have no evidence for quantization at multiples of 72 km s^{-1}, but the more basic result is that there are few pairs altogether with $\Delta V \geq 100$ km s^{-1}. We cannot comment on "subquantization effects" with a unit of 24 km s^{-1} (Tifft 1988), since much better statistics would be required for finer binning, and because the ΔV distribution changes with r_p.

5.2. *Effect of Isolation with Respect to Galaxies in the Redshift Catalogs*

It would be of interest to know how the distribution of ΔV for a pair is affected by (1) other companions within ~ 1 Mpc and by (2) the overall galaxy number density on slightly larger scales. For instance, a simple approach towards "cosmic virial equilibrium" (Gott & Rees 1975; Peebles 1976) would suggest

that ΔV tends to increase with local density. On another scenario (Ostriker & Cowie 1980), ΔV would depend more on previous energetic explosions than on density. We hope to study the second factor in the future but already have some data on the first factor for our northern sample where we have H I velocities for all pairs regardless of isolation.

To check on the effects of isolation, we plot in Figure 4 the velocity difference histograms for the northern samples. Figure 4*a* is for pairs isolated to 0.25 Mpc and 300 km s^{-1}, Figure 4*b* is for pairs isolated to 0.35 Mpc and 300 km s^{-1}, and Figure 4*c* is for the "isolated pairs," isolated to 0.75 Mpc and 300 km s^{-1}. The most notable feature is that, as the isolation criterion becomes more stringent, pairs are preferentially lost from the large-velocity tail of the histogram. The median velocity difference is 78.5 km s^{-1} for the sample isolated to (0.25 Mpc, 300 km s^{-1}), 45.6 km s^{-1} for the sample isolated to (0.35 Mpc, 300 km s^{-1}), and 28.5 km s^{-1} for the sample isolated to (0.75 Mpc 300 km s^{-1}).

To quantify the qualitative impression that increasing stringency of the isolation criterion causes pairs to be selectively lost from the tail of the distribution, we fitted a model consisting of the sum of a Gaussian plus a constant background (i.e., a straight line) to the histograms in Figure 4. The width of the Gaussian is unaffected by isolation, as expected. In order of increasing stringency of the isolation criterion, the half-width at full maximum of the fitted Gaussian is 27 ± 4 km s^{-1}, 28 ± 4 km s^{-1}, and 27 ± 4 km s^{-1}. The background value, however, decreases by a factor of 2 from the least stringently isolated sample to the most stringently isolated sample.

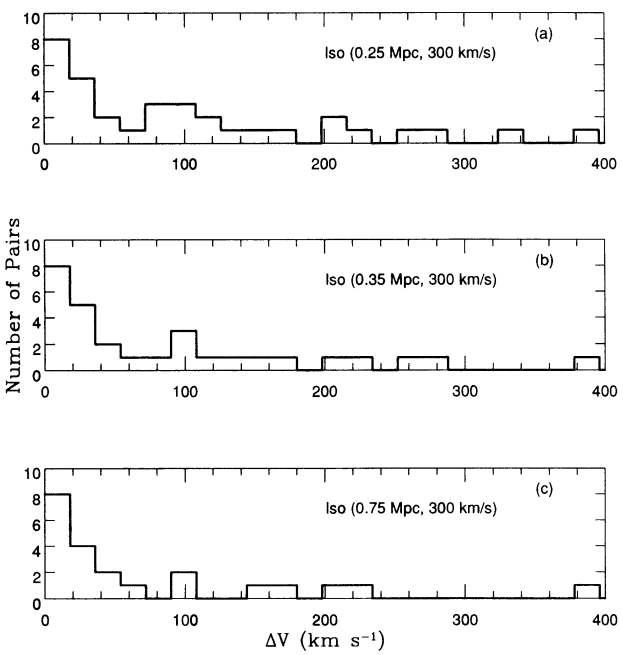

FIG. 4.—(*a*) Histogram of the velocity distribution for pairs of galaxies from the Arecibo sample. The width of each bin is 18 km s^{-1}. The isolation criteria used is that there should be no third galaxy within 0.25 Mpc and 300 km s^{-1} of either galaxy in the pair. (*b*) Histogram of the velocity distribution for pairs of galaxies from the Arecibo sample. The width of each bin is 18 km s^{-1}. The isolation criteria used is that there should be no third galaxy within 0.35 Mpc and 300 km s^{-1} of either galaxy in the pair. (*c*) Histogram of the velocity distribution for pairs of galaxies from the Arecibo sample. The width of each bin is 18 km s^{-1}. The isolation criteria used is that there should be no third galaxy within 0.75 Mpc and 300 km s^{-1} of either galaxy in the pair, i.e., "isolated sample."

Isolation is hence a strong determining factor of galaxy velocities, and isolated galaxies have extremely small velocity differences. There may be a similar dependence on overall galaxy number density. Rivolo & Yahil (1981), using the RSA catalog with restriction to low densities found appreciably larger "typical values" for ΔV (100 km s^{-1}) than our study ($\sim$30 km s^{-1}). Part of the difference stems from the larger redshift errors in the RSA, but part may be due to the density effect.

5.3. *Effect of Isolation with Respect to Galaxies Not in the Redshift Catalogs*

Throughout the above discussion we have used the term "isolation" only in reference to galaxies in the redshift catalog. If a pair has no neighbors in the catalog, it is regarded as being "isolated." An "isolated" pair could well have a companion galaxy just slightly fainter than the catalog limit. (For example, the Local Group excluding M33 and the LMC would qualify as an "isolated pair" if it were displaced to a redshift $\geq$1500 km s^{-1}.) How often does this happen, and how does it affect our results? These questions can be firmly answered only once deeper complete redshift catalogs are available. However, some preliminary indications can be obtained by using the redshift data currently available for fainter galaxies.

For all the galaxies in Table 2 (i.e., those with velocity difference less than 200 km s^{-1} and no other catalog galaxy within 0.75 Mpc and 300 km s^{-1}), we searched the NED[3] database for fainter companion galaxies with a projected separation less than 0.75 Mpc and a velocity difference less than 300 km s^{-1}. For 14 of the 32 pairs we found at least one companion which also had brightness within 2 mag of the primary galaxy. In one case, UGC 12815, the companion (UGC 12813) is 1.5 mag fainter than the primary galaxy and just 0.02 mag fainter than the magnitude limit of the CfA catalog. For the diameter-limited southern catalog, the situation is even more complex. One of the pairs, 540G10-540G6, has a third galaxy of comparable brightness to the fainter pair member, but which is so compact that it is neither in the ESO (Lauberts 1982) nor the SSRS catalogs.

The median of the velocity difference of the 14 pairs with companions in the NED database is 34 km s^{-1}, which is slightly, and not significantly, larger than the value of 28 km s^{-1} for the 18 pairs with no companions in the NED database. This difference in median ΔV is not statistically significant in view of the small numbers, although the sign is as suggested by § 5.2, i.e., we expect the most highly isolated pairs to have a smaller median ΔV.

6. SOME SIMPLE DYNAMICAL MASS FORMULAE

In this section we gather together a list of relatively simple formulae for the dynamical mass of galaxy pairs. We apply these formulae to our observed pairs and discuss the results in the next section.

The first formula is the indicative mass formula from Faber and Gallahager (1979):

$$M_{\rm ind} = \frac{16}{3\pi G} \Delta V^2 r_p ,$$

[3] The NASA/IPAC Extragalactic Database (NED) is operated by the Jet Propulsion Laboratory, California Institute of Technology, under contract with the National Aeronautics and Space Administration.

or

$$M_{\rm ind} = 4 \times 10^{12}\, M_\odot \left(\frac{\Delta V}{100\ {\rm km\ s^{-1}}}\right)^2 \left(\frac{r_p}{1\ {\rm Mpc}}\right). \quad (1)$$

Note that this assumes virialized orbits, which is not the case for our pairs, since the crossing time $\sim r_p/\Delta V$ is comparable to the Hubble time (see § 7).

If we assume that each galaxy has an isothermal halo which extends out to large separations, then the mass of each halo is given by

$$M_{\rm halo} = \frac{W^2 \times r_{\rm halo}}{4G},$$

where W is the full rotation width (i.e., twice the circular velocity) of the galaxy and $r_{\rm halo}$ is the size of the halo. Numerically,

$$M_{\rm halo} = 5 \times 10^{12}\, M_\odot \left(\frac{W}{300\ {\rm km\ s^{-1}}}\right)^2 \left(\frac{r_{\rm halo}}{1\ {\rm Mpc}}\right). \quad (2)$$

Another fiducial mass is that of a homogeneous sphere of radius r with density just equal to the critical density. This is

$$M_{\rm crit} = \frac{r^3 H_0^2}{2G},$$

or

$$M_{\rm crit} = 6 \times 10^{11}\, M_\odot \left(\frac{H_0}{75\ {\rm km\ s^{-1}\ Mpc^{-1}}}\right)^2 \left(\frac{r}{1.0\ {\rm Mpc}}\right)^3. \quad (3)$$

Finally, the total mass of a system of two particles which were moving apart at the Hubble expansion rate at early epochs but which have been slowed down by mutual gravitation and have just reached turn around at a separation of r at the current epoch ($\Delta V = 0$ now), is given by

$$M_{\rm ta} = \frac{9\pi^2}{32} \times \frac{r^3 H_0^2}{G}$$

or

$$M_{\rm ta} = 4 \times 10^{12}\, M_\odot \left(\frac{H_0}{75\ {\rm km\ s^{-1}\ Mpc^{-1}}}\right)^2 \left(\frac{r}{1.0\ {\rm Mpc}}\right)^3. \quad (4)$$

We have assumed a flat $\Omega = 1$ universe. Note that $M_{\rm ta}$ and $M_{\rm crit}$ differ only by the numerical factor.

7. FURTHER STATISTICS AND COMMENTS ON MASS ESTIMATES

We consider here only those pairs which are most likely to be physically associated with one another, i.e., pairs from both the Arecibo and the Parkes samples, which are isolated to 0.75 Mpc, 300 km s^{-1} and which are in the small-ΔV peak (velocity differences less than 100 km s^{-1}). Since the pairs can have separations of up to 1.0 Mpc, they are not *isolated* binary galaxies in the strictest sense. However, as we noted in § 4, the exact isolation criterion used has relatively little effect on the properties of pairs in the small-ΔV peak. There are 27 pairs in this sample, and they have a median value of the projected separation, r_p, of 553 kpc × (75 km s^{-1} Mpc^{-1}/H_0). With our (somewhat arbitrary) velocity difference cutoff of 100 km s^{-1}, the median value of ΔV is 26.2 km s^{-1}. For a cutoff of 200 km s^{-1}, the median is 28.5.

7.1. *Further Statistics*

In addition to the average properties over the sample, it is also interesting to examine the shape of the distribution of pair properties. As mentioned above, if halos are extensive, then the degree of overlap plays a large role in determining the relative velocity of pairs. In order to facilitate comparisons with future theoretical models which include dynamical friction, we show in Figure 5 the histogram of the dimensionless ratio $\Delta V/W_0$ for all pairs which are isolated to (0.75 Mpc, 300 km s^{-1}) and have $\Delta V < 100$ km s^{-1} (*solid histogram*), or $\Delta V < 200$ km s^{-1} (*dashed histogram*). The median value of $\Delta V/W_0$ is 0.08. A relatively small value of $\Delta V/W_0$ could arise for three reasons: (1) The halos are large enough to overlap and the resulting dynamical friction has decreased the relative velocity of the pair; (2) the halos are quite small, leading to fall-off in the orbital speed with increasing distance; and (3) the pair is near "turn-around" (see § 7.2).

The velocity difference of the isolated pair sample as a function of projected separation is shown in Figure 6. There is a large scatter but also perhaps a slight trend for decreasing velocities with increasing projected separation. However, this is not, statistically significant, the correlation coefficient between ΔV and r_p is -0.23, corresponding to a nominal statistical significance of 75%.

Figure 7 is a plot of velocity difference against luminosity. The luminosity is based on the total blue magnitude as listed in the RC3 (de Vaucouleurs et al. 1992). Once again there is a large scatter and perhaps a slight trend for increasing velocity differences with increasing luminosity, which can be seen by dividing the sample into thirds. For pairs with $L_{\rm tot} < 1.3 \times 10^{10}\ L_\odot$, the median velocity difference is $\Delta V = 26.8$ km s^{-1}. For pairs with $1.3 \times 10^{10}\ L_\odot < L_{\rm tot} < 2.0 \times 10^{10}\ L_\odot$, the median velocity is $\Delta V = 25.0$ km s^{-1} and for pairs with $L_{\rm tot} > 2.0 \times 10^{10}\ L_\odot$, the median velocity is $\Delta V = 45.6$ km s^{-1}. The correlation coefficient between ΔV and $L_{\rm tot}$ is 0.52, corresponding to a nominal statistical significance of 99%.

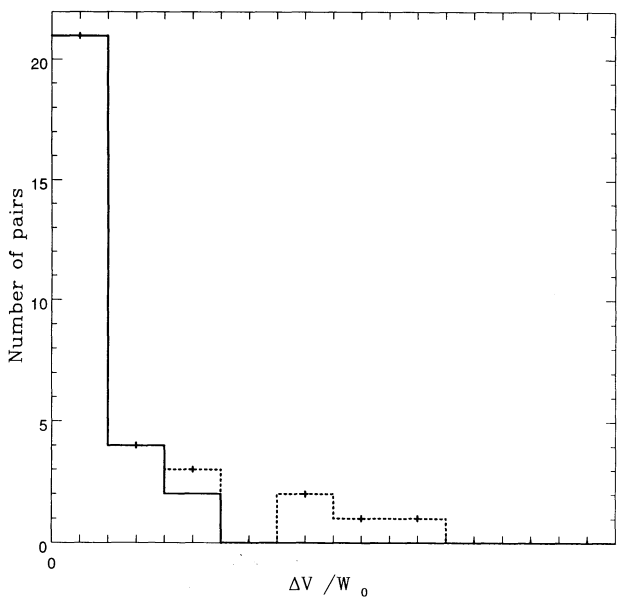

FIG. 5.—Histogram of $\Delta V/W_0$ for pairs of galaxies from the "isolated sample," and with $\Delta V < 100$ km s^{-1} (*solid line*) and with $\Delta V < 200$ km s^{-1} (*dashed line* and *crosses*). Both ΔV and W_0 are in km s^{-1}; the binning interval is 0.1.

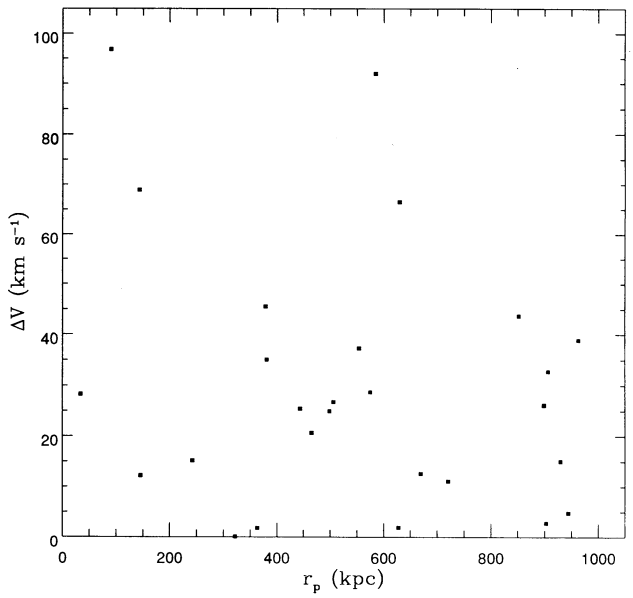

FIG. 6.—The velocity difference against projected separation of the pairs from the "isolated sample" and with $\Delta V < 100$ km s^{-1}.

If one assumes a constant mass-to-light ratio, different pairs can be put on the same scale by dividing the indicative mass ($M_{\rm ind}$ in eq. [1]) by the total luminosity of the pair. Equivalently, one could scale the projected separation inversely by the total luminosity. We define this luminosity-weighted projected separation as follows: $r_k = [r_p(\text{kpc})/L_{\rm tot}] \times 9.2 \times 10^9\ L_\odot$. r_k is in units of kpc. The average total luminosity of the pairs is $9.2 \times 10^9\ L_\odot$. ΔV as a function of r_k is shown in Figure 8. The superposed curve is for an indicative mass of $0.45 \times 10^{12}\ M_\odot$. Recall that the indicative mass assumes virialization, which is unlikely to be true for our pairs.

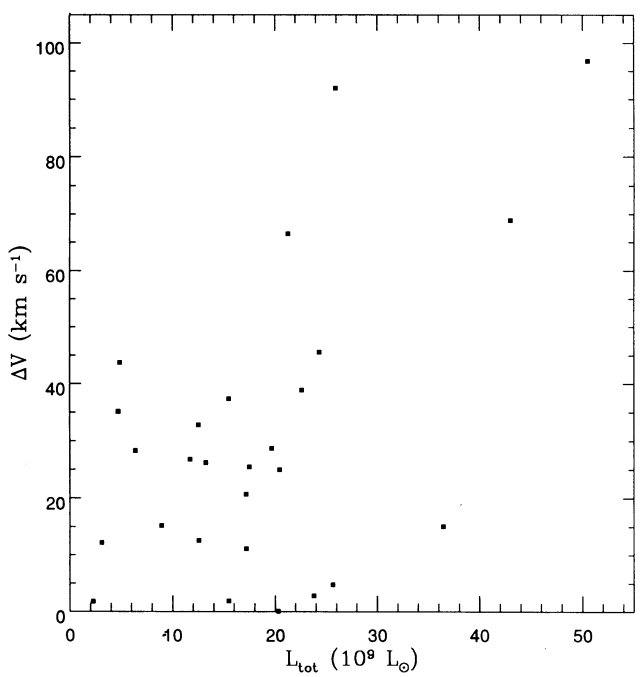

FIG. 7.—The velocity difference against total luminosity for the pairs from the "isolated sample" and with $\Delta V < 100$ km s^{-1}.

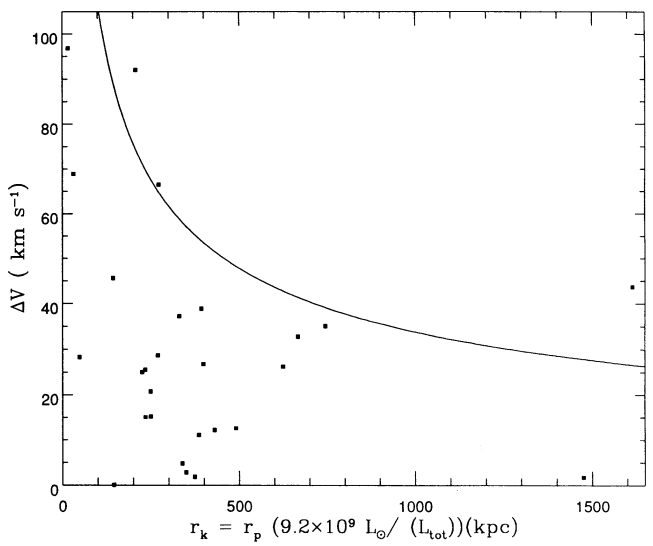

FIG. 8.—The velocity difference of the pairs from the "isolated sample" and with $\Delta V < 100$ km s^{-1} as a function of the luminosity weighted projected separation. The superposed curve is for an indicative mass of $0.45 \times 10^{12}\ M_\odot$.

7.2. *Discussion of Mass Estimates*

Using our median values for r_p and ΔV, we find for $M_{\rm ind}$ in equation (1) and for $M_{\rm ta}$ in equation (4), with r replaced by r_p the following numerical values:

$$M_{\rm ta} \simeq 5 \times M_{\rm ind} \simeq 0.7 \times 10^{12}\, M_\odot \left(\frac{H_0}{75\ \text{km s}^{-1}}\right)^{-1} . \quad (5)$$

The ratio of these two mass indicators is related to a dimensionless quantity:

$$\zeta \equiv \frac{\Delta V}{H_0 \times r_p} \simeq \frac{\Delta V}{V_{\rm syst}} \times \frac{1\ \text{rad}}{\theta_p} , \quad (6)$$

where θ_p is the angular separation of the galaxy pair. For our sample, the median value of ζ is 0.67, independent of the value of H_0. The derivation of equation (1) for the "indicative mass" estimator $M_{\rm ind}$ assumes time for executing many orbits, i.e., $\zeta \gg 1$. This is not the case for our median pairs, so that $M_{\rm ind}$ is of little use, but $M_{\rm ta}$ is of some relevance, as can be seen from the following arguments.

Since ζ is not very large, one cannot be sure of having a bound pair, but the pair must be physically associated because of the following inequality: If it were not, the rms value ΔV would be $(2\ \sigma)^{1/2}$ where σ is the (one-dimensional) "cosmic random thermal velocity," i.e., the small-scale velocity dispersion for an individual galaxy. Strauss, Cen, & Ostriker (1993) estimate $\sigma \geq 200$ km s^{-1}, so that $\Delta V \ll (2)^{1/2}\ \sigma$, and the two galaxies in a pair must have formed together (unless the estimates are grossly in error, or do not hold for scales as small as 1.0 Mpc), probably at some smaller separation than they have now. Let $\zeta_{\rm tot}$ be the quantity equivalent to equation (6), but with the total velocity difference and separation instead of ΔV and r_p. If galaxy masses M satisfied the inequality $M \ll M_{\rm ta}$, the pair would expand with pure Hubble flow, i.e., $\zeta_{\rm tot} = 1$. The quantity ζ would fluctuate from pair to pair, but ΔV and r_p would be positively correlated (approximately linearly). Figure 6 shows that this is not the case, i.e., the gravitational attraction between the two galaxies has altered the Hubble flow. If one had $\Delta V = \zeta = 0$ for each pair, (i.e., "turn-around"), one

would have $M \sim M_{ta}$ and the median mass would be $\sim 0.7 \times 10^{12}\ M_\odot\ \sec^3 \alpha$, where α is the inclination of the pair separation to the line of sight. Assuming $\zeta_{tot} \sim \zeta \sim 0.7$ one can integrate the equations of motion to get numerical values for the total mass (Kahn & Woltjer 1959; Peebles 1971). We find $M \sim 0.4 \times M_{ta}$ if the present epoch is before the first turn around (at maximum separation), $M \sim 1.4 \times M_{ta}$ if it is after the first maximum and before the first minimum separation, $M \sim 7 \times M_{ta}$ for the next case, etc.

Zaritsky et al. (1993) have studied faint satellites of spiral galaxies with separations r_p somewhat smaller than ours and find a ΔV somewhat larger. Their values for ζ are thus larger, M_{ind} a more reliable estimator, and they find typical galaxy masses of order $2 \times 10^{12}\ M_\odot$. These masses are thus of roughly the same order as our 1.4 $\sec^3 \alpha M_{ta}$. If one assumed isothermal dark matter halos extending to a radius of ~ 0.5 Mpc, equation (2) gives a mass $M_{halo} \sim 3 \times 10^{12}\ M_\odot$. In the CfA plus SSRS catalogs as a whole, there is one galaxy in a sequence of radius 4 Mpc on the average (Charlton & Salpeter 1991). For $M_{halo} \sim 3 \times 10^{12}\ M_\odot$, the contribution to the cosmological density parameter would then be $\Omega_{halo} \sim 0.1$.

8. CONCLUSIONS

The dynamics of pairs of galaxies chosen from the CfA and SSRS catalogs is analyzed and new H I data for these pairs obtained at both Arecibo and Parkes observatories is presented.

The velocity difference distribution of wide isolated galaxy pairs shows no evidence for the existence of a preferred value of 72 km s^{-1}. The distribution is instead peaked at the origin and monotonically decreasing with increasing velocity difference. This confirms the suggestion by Schneider & Salpeter (1992) that the nonmonotonicity of the velocity distribution of early samples of galaxies is a consequence of a selection bias.

The distribution of ΔV for galaxy pairs in low density regions is found to have two components, a peak around zero and a tail extending to larger velocity differences. The tail of the ΔV distribution has a strong dependence on the degree of isolation. As the stringency of the isolation criterion is increased, pairs are preferentially lost from the tail of the distribution. The width of the peak around zero, on the other hand, has little dependence on the isolation criterion.

Isolated wide pairs of galaxies have extremely small velocity differences. Paris with separations of ~ 1.0 Mpc have a median velocity difference of ~ 30 km s^{-1}. The velocity difference of isolated pairs decreases with increasing projected separation. The 30 km s^{-1} characteristic velocity difference for our sample of wide pairs is roughly half the typical median velocity difference of 70 km s^{-1} of either samples of more compact pairs.

Masses cannot be derived reliably, but a plausible mass indicator that gives a characteristic mass for our galaxy pairs is of the order $10^{12}\ M_\odot$ This is consistent with the estimated mass of the local group and also with the mass estimated for a sample of spiral galaxies by the dynamics of their faint satellites by Zaritsky et al. (1993).

We would like to thank J. Huchra for providing a computer readable version of the CfA catalog, and L. da Costa and P. Pellegrini for providing a computer-readable version of the SSRS. We are also grateful to M. P. Haynes and R. Giovanelli for permitting us to use their compilation of largely unpublished H I observations and also for conducting some of the observations at Arecibo on our behalf. We would also like to thank them for several illuminating discussions, and R. Giovanelli especially for suggesting the velocity measurement algorithm used in this work. Some of the Arecibo observations were kindly conducted by C. Pantoja, and all the telescope operators at the Arecibo observatory provided cheerful assistance throughout. We also thank M. Ashby, J. Charlton, S. Gelato, S. Schneider, and W. G. Tifft for useful discussions and comments, and J. Charlton especially for providing the selection functions for the CfA and SSRS catalogs. J. Navarro kindly donated useful software. We would like to thank R. D. Ekers for hospitality at the CSIRO-ATNF, Robina Otrupcek and D. Milne for assistance with the Parkes observations, and L. L. Staveley-Smith for assistance with the conversion of the Parkes data to a standard format. This work was supported in part by the National Astronomy and Ionsphere Center, which is administered by Cornell University under a cooperative agreement with the National Science Foundation, and in part by NSF grant AST 91-19475. Part of J. N. C.'s travel expenses to Parkes were funded by a grant from the Astronomical Society of New York. This research has made use of the NASA/IPAC Extragalactic Database (NED) which is operated by the Jet Propulsion Laboratory, Caltech, under contract with the National Aeronautics and Space Administration.

REFERENCES

Charlton, J., & Salpeter, E. E. 1991, ApJ, 375, 517
Chengalur, J. N., Salpeter, E. E., & Terzian, Y. 1993, in preparation
Cocke, W. J., & Tifft, W. G. 1983, ApJ, 268, 56
da Costa, L. N., Pellegrini, P. S., Davis, M., Meiksin, A., Sargent, W. L. W., & Tonry, J. L. 1991, ApJS, 75, 935
da Costa, L. N., et al. 1988, ApJ, 327, 544
de Vaucouleurs, G., de Vaucouleurs, A., Corwin, H. G., Buta, R. J., Paturel, G., & Fouque, P. 1992, Third Reference Catalogue of Bright Galaxies (New York: Springer-Verlag) (RC3)
Faber, S. M., & Gallahager, J. S. 1979, ARA&A, 17, 135
Gott, J. R., III, & Rees, M. 1975, A&A, 45, 365
Haynes, M. P., & Giovanelli, R. 1992, private communication
Huchra, J. P., Davis, M., Latham, D. W., & Tonry, J. 1983, ApJS, 52, 89
Huchra, J. P., & Geller, M. J. 1982, ApJ, 257, 423
Karachentsev, I. D. 1972, Comm. Spec. Ap. Obs. USSR, 7, 1
Kahn, F. D., & Woltjer, L. 1959, ApJ, 130, 705
Lauberts, A. 1982, The ESO/Uppsala Survey of the ESO (B) Atlas (Garching-bei-Muñchen: European Southern Observatory)
Newman, W. I., Haynes, M. P., & Terzian, Y. 1989, ApJ, 344, 111
Ostriker, J., & Cowie, L. L. 1980, ApJ, 243, L127
Page, T. 1952, ApJ, 116, 63
Peebles, P. J. E. 1976, ApJ, 205, L109
Peebles, P. J. E. 1971, Physical Cosmology (Princeton: Princeton Univ. Press)
Peterson, S. D. 1979, ApJ, 232, 20
Rivolo, A. R., & Yahil, A. 1981, ApJ, 251, 477
Schneider, S. E. 1985 PhD thesis, Cornell Univ.
Schneider, S. E., Helou, G., Salpeter, E. E., & Terzian, Y. 1986, AJ, 92, 742
Schneider, S. E., & Salpeter, E. E. 1992, ApJ, 385, 32 (SS)
Schweizer, Y. L. 1987, ApJS, 64, 427
Sharp, N. A. 1990, ApJ, 354, 418
Soares, D. S. L. 1990, A&A, 232, 50
Strauss, M. A., Cen, R., & Ostriker, J. P. 1993, ApJ, 408, 389
Tifft, W. G. 1977, ApJ, 211, 31
———. 1980, ApJ, 236, 70
———. 1982a, ApJ, 257, 442
———. 1982b, ApJ, 262, 44
———. 1988, New Ideas in Astronomy (Cambridge: Cambridge Univ. Press)
Tift, W. G., & Cocke, W. J. 1987, S&T, 73, 19
———. 1989, ApJ, 336, 128
Turner, E. L. 1976, ApJ, 208, 20
van Moorsel, G. A. 1982 PhD thesis, Univ. of Groningen
White, S. D. M. 1981, MNRAS, 189, 831
White, S. D. M., Huchra, J., Latham, D., & Davis, M. 1983, MNRAS, 203, 701
Zaritsky, D., Rodney, S., Carlos, F., & White, S. D. M. 1993, ApJ, 405, 464